R.O. Chalmers, Commemorative Papers (Mineralogy, Meteoritics, Geology)

Edited by

Lin Sutherland

Zeolites from a New Locality at Ben Lomond, New England Region, New South Wales

BRIAN M. ENGLAND

Analytical Technology Group, Environmental Research, BHP Research, Newcastle Laboratories, PO Box 188, Wallsend, NSW 2287, Australia

ABSTRACT. A roadside quarry on the New England Highway near Ben Lomond in the New England Region of New South Wales has revealed an interesting association of zeolites and other secondary minerals lining vesicles in Tertiary basalt. The zeolites present (chabazite, phillipsite and natrolite) are those characteristic of a silica-undersaturated (alkaline) environment. Associated secondary minerals include radiate globular saponite, calcite and aragonite. The calcite is present in a number of different habits, each showing a different response to ultraviolet light and the aragonite also shows a diverse range in morphology. Zonal distribution of the zeolite species is pronounced with the zoning centred around what appear to have been hydrothermal spring conduits. Two distinct episodes of mineralisation are evident, an early deuteric suite formed during initial cooling of the basalt and a later suite (including chabazite and radiate globular saponite) deposited by a further influx of hydrothermal fluids associated with subsequent proximal hot spring activity. The basalt at this locality has undergone extensive hydrothermal alteration.

ENGLAND, B.M., 1992. Zeolites from a new locality at Ben Lomond, New England Region, New South Wales. Records of the Australian Museum Supplement 15: 55–72.

A small quarry (Fig.1) beside the New England Highway 28 km north of Guyra, excavated during road reconstruction in 1987, has intersected an extensively altered vesicular Tertiary basalt. Vesicles exposed in the quarry face reach 15 cm across and are lined principally with chabazite showing a variety of multiply-twinned (phacolite) habits. Other minerals present at the locality but not always directly associated with the chabazite include saponite (smectite group), aragonite, phillipsite, natrolite and calcite. Crystal size is generally quite small (less than 2 mm), although chabazite crystals to 1.5 cm diameter have been observed. The larger crystals tend to occur in the smaller vesicles.

The locality displays a number of unusual features including at least two episodes of mineralisation and diverse aragonite and calcite morphologies, the latter showing an equally diverse range of responses to ultraviolet light.

The small size of many of the crystals and the various combinations of species present make this one of the finest localities in Australia for zeolite micromounts. Due to extensive alteration the basalt is unusually brittle, making the collection and trimming of specimens easy.

Geology and Occurrence of Zeolites and Associated Secondary Minerals

The locality appears to represent the amygdaloidal top of a massive flow at the base of an extensive sequence of Tertiary basalts extending through the New England region.

The zeolites and associated minerals show a distinct zonation within the exposed basalt over a vertical distance of around 3 m. Near the top of the exposure the basalt has undergone extensive hydrothermal alteration to massive saponite and the vesicles are lined with druses of coarsely crystallised chabazite, with later calcite as the only associated mineral. Lower down, smaller quantities of chabazite are accompanied by an abundance of earlier phillipsite and less extensive alteration of the basalt, with only the mesostasis replaced by saponite. However, in this zone the saponite begins to appear in vesicles as distinct radiate globules ('spherulites' of Lebedev, 1967) rather than the more typical massive material. Adjacent to the base of the exposure, phillipsite-natrolite-radiate globular saponite-calcite associations predominate. Here chabazite is the penultimate species to crystallise (prior to calcite) and only occasional vesicles contain significant amounts of this zeolite. The basalt in all three zones contains abundant disseminated ilmenite crystals to 30 μm in diameter.

Half way down the quarry face and roughly separating the chabazite and phillipsite zones in the basalt is a series of moderately large and laterally extensive lensoidal cavities, each up to a metre in cross-section (Fig.2). These have fine ash and lapilli at their base and also contain layered, and occasionally cross-bedded, sedimentary material in which major thompsonite and minor chabazite were identified by X-ray powder diffraction (XRD). Their roofs are composed of stalactitic masses of finely crystallised chabazite and intense hydrothermal alteration at the periphery of the cavities has resulted in extensive development of massive saponite. The basalt in the vicinity of these cavities shows considerable disruption to normal flow patterns, with vesicle lineation varying from near horizontal to vertical over lateral distances of a few metres. The probable significance of these features is discussed later in this paper.

Description of the Vesicle Minerals

Examination of associations in over 100 vesicles from the lower part of the exposure under a binocular microscope revealed the paragenesis shown in Table 1 (Appendix). Most of the minerals present were initially identified by XRD carried out by Ross Pogson of the Australian Museum. The minerals are described in alphabetical order.

Fig.1. Roadside quarry in amygdaloidal Tertiary basalt on the New England Highway, 28 km north of Guyra, NSW. Photograph by the author.

Aragonite $CaCO_3$ (Aragonite Group)

Aragonite is occasionally present as colourless to pale yellow water-clear crystals with a sub-conchoidal fracture, associated with earlier phillipsite and natrolite and later radiate globular saponite in vesicles. Crystals show a variety of prismatic and symmetrically-distorted habits, comprising m{110} and b{010} terminated by k{011} and are usually less than 3 mm in length, although radiating sprays with individual crystals to 1 cm have been found alone in vesicles at the southern end of the quarry. The b{010} faces are usually either very small or entirely absent. Simple contact twinning on {110} is common and often repeated, with a re-entrant groove running the full length of crystals in place of the juxtaposed b(010) and b(010) faces of the two individuals.

Symmetrical distortion of the m{110} and k{011} forms has produced a variety of unusual crystal habits (Fig.3). Quite commonly, gross inequality in diametrically opposite pairs of m faces has resulted in very thin blade-like crystals, tabular on m(110). The k faces are also commonly offset, occasionally to the total exclusion of either (011) or ($0\bar{1}1$), giving a pseudomonoclinic bladed habit.

The aragonite crystals show a strong pale yellow fluorescence under both long and short wave ultraviolet light, with a strong but very brief yellow phosphorescence after excitation with short wave ultraviolet. The responses are more intense towards the terminations of the crystals.

Calcite $CaCO_3$ (Calcite Group)

One of the most unusual features of this locality is the number of different calcite habits present in vesicles. While not all habits could be precisely located within the paragenesis using the samples available, marked differences in morphology and response to ultraviolet light strongly suggest distinctly separate episodes of crystallisation. At least eight variations in calcite morphology have been recognised and these are described below in their inferred order of crystallisation. The various crystal forms have not been positively identified and the drawings in Figure 5A-D represent the morphologies which most closely resemble the observed crystals.

1. Irregular, transparent, amber-coloured sharp needles to 8 mm in length (Fig.4) deposited after saponite but before phillipsite. These are heavily fluted and may represent early aragonite since reverted to calcite. No definite forms could be recognised on any of the crystals. These crystals show a strong mustard-yellow fluorescence and brief yellow phosphorescence under both long and short wave ultraviolet light.

2. Pale milky-yellow to amber radiating groups of acute rhombohedra to 5 mm across (Fig.5A) deposited after the needle calcite but before phillipsite. These

Fig.2. Large lensoidal cavities exposed in the quarry face. Depth of section is approximately 3 m. Photograph by the author.

crystals occur in the same vesicles as type 1 and show the same ultraviolet response.

3. Water-clear amber scalenohedra to 1 cm in length terminated by acute rhombohedra (Fig.5B). These usually follow natrolite but precede radiate globular saponite, although occasionally this habit was seen deposited on chabazite. Crystals show pale yellow fluorescence and brief yellow phosphorescence under both long and short wave ultraviolet light.

4. Very acute trigonal pyramids up to 2 mm in length (Fig.5C), crystallised after phillipsite but before radiate globular saponite. The relationship between this habit and type 3 above could not be determined from the specimens examined so far. Crystals show bright pinkish-yellow fluorescence under both long and short wave ultraviolet light but no phosphorescence.

5. White to amber, slightly modified acute rhombohedra (Fig.5D) deposited after phillipsite but before chabazite. Crystals average around 2 mm in maximum dimension. The relationship between this habit and types 3 and 4 described above could not be determined from the specimens examined. These crystals show a pink fluorescence under both long and short wave ultraviolet light and a distinctly brighter pink phosphorescence.

6. Very fine crystalline material deposited in hemispherical concentrations within the base of acicular natrolite groups and occasionally extending outwards along individual natrolite crystals. This material shows a very bright creamy yellow fluorescence under both long and short wave ultraviolet light and an astonishingly persistent bright yellow phosphorescence after removal of specimens from the excitation source.

7. Incipient to rare advanced radiate globular forms ('spherulites' of Lebedev, 1967) which reach a maximum dimension of 2 mm. While the globular habit from this locality has not been microanalysed due to a shortage of suitable material, detailed investigation of identical crystals from Kulnura, NSW has shown this

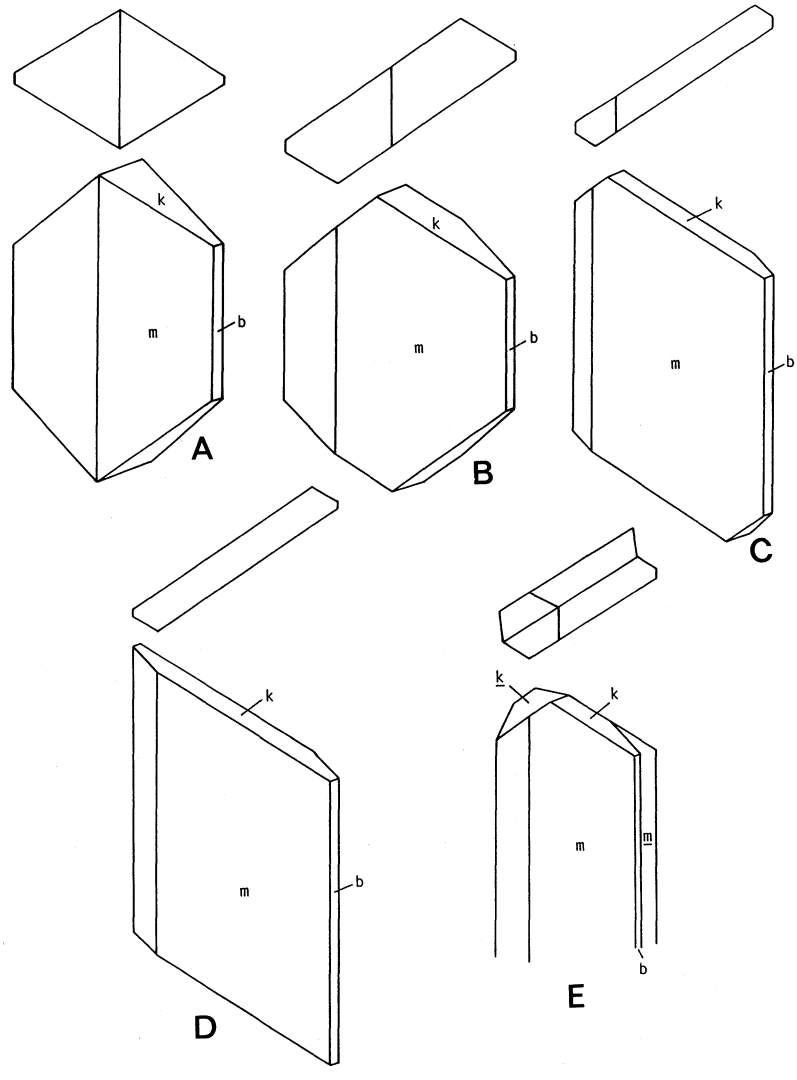

Fig.3. Habit variations in aragonite crystals from Ben Lomond, showing typical distortions produced by the inequality between diametrically opposite pairs of m faces and offsetting of k faces (Drawings B-D). A typical contact twin on (110) is shown in Drawing E. Drawings by the author.

habit to have developed by repeated splitting of the form r{10$\bar{1}$1} along the rhombohedral cleavage directions due to sectorial enrichment in $MgCO_3$ and to a lesser extent $FeCO_3$ (England, 1984). The more magnesium and/or iron absorbed by the calcite, the greater is this splitting effect. This causes the lateral corners of the rhombohedron to curl alternately up and down towards the c-axis, producing a variety of morphologies ranging from simple saddle-shaped crystals to complex spherical habits with an internal radiate structure. These crystals were deposited after chabazite and represent the last material to crystallise

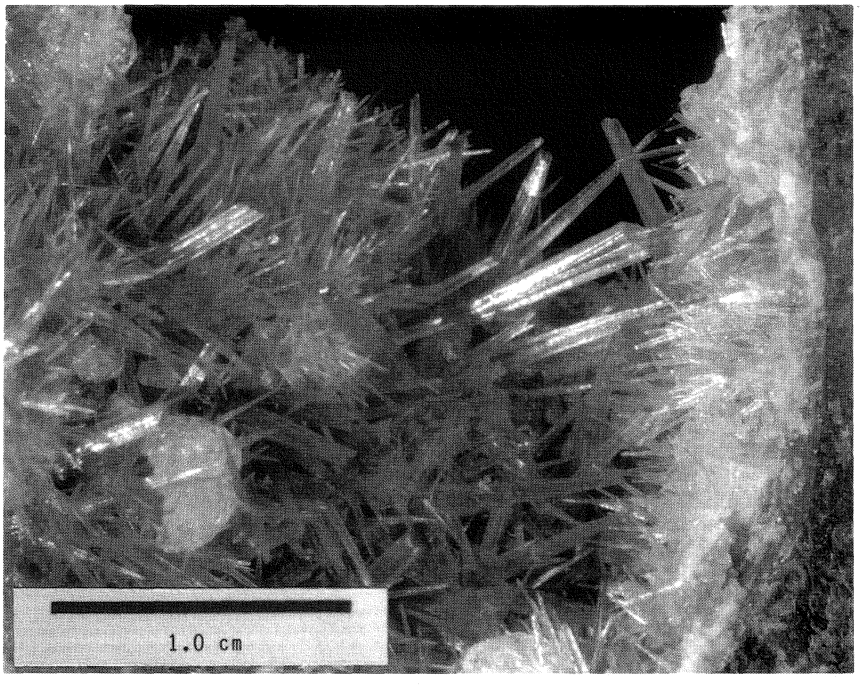

Fig.4. Transparent amber-coloured needles of calcite to 8 mm in length lining a vesicle. Photograph by the author.

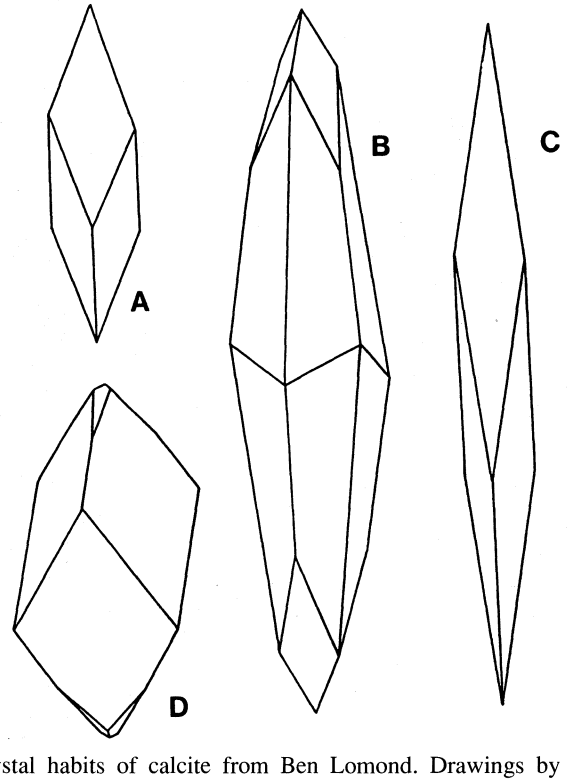

Fig.5. Variation in the crystal habits of calcite from Ben Lomond. Drawings by the author (modified from Goldschmidt, 1913).

in the vesicles. Specimens show a bright pink fluorescence under both long and short wave ultraviolet light, but no phosphorescence.

8. White powdery coatings on earlier species. These show no obvious response to ultraviolet light.

The distribution of calcite in different habits throughout the paragenesis may be a result of gradual changes in the physico-chemical nature of the hydrothermal system from which the secondary minerals were deposited. The particular calcite habit produced in each case would be dependant on the temperature of the system and the concentration of impurity atoms at the time of crystallisation (Leitmeier, 1910, 1915), the latter also probably explaining the differences in reaction to ultraviolet light. The occurrence of globular habits and powdery coatings late in the paragenesis may represent either residual calcium carbonate trapped within the

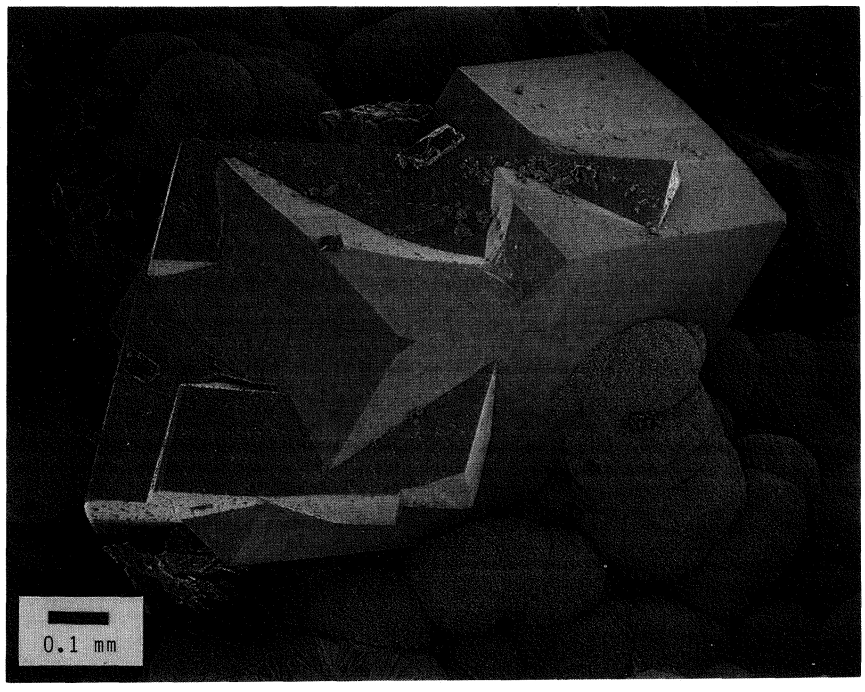

Fig.6. Interpenetrant chabazite rhombohedra twinned on the c-axis with radiate globular saponite. Scanning electron micrograph, secondary electron image. Author's specimen and micrograph.

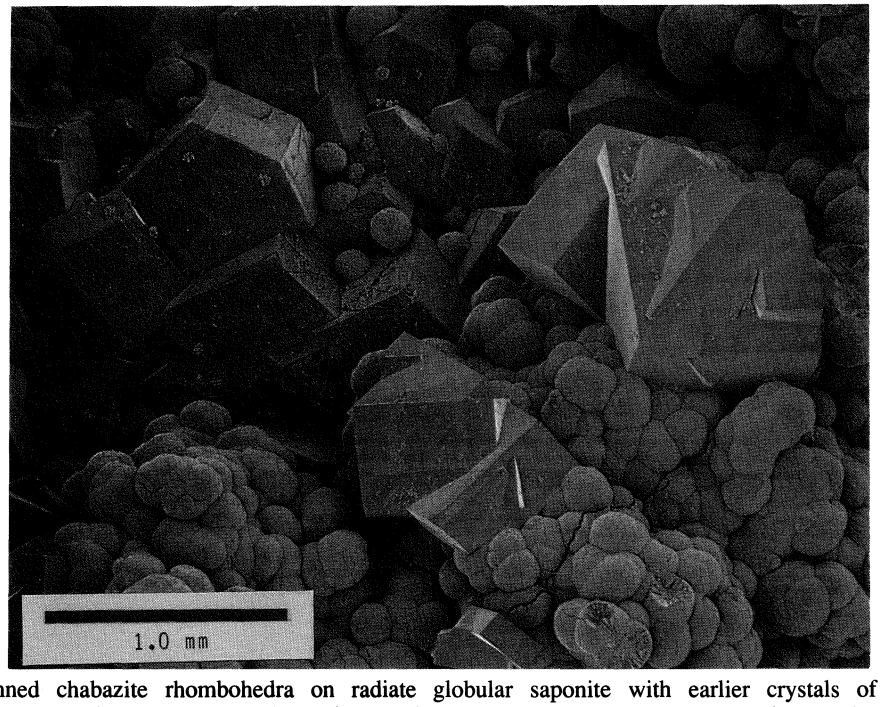

Fig.7. Twinned chabazite rhombohedra on radiate globular saponite with earlier crystals of phillipsite. Scanning electron micrograph, secondary electron image. Author's specimen and micrograph.

vesicles or material deposited from recent groundwater movements.

Chabazite $CaAl_2Si_4O_{12}.6H_2O$ (Zeolite Group)

Chabazite is ubiquitous throughout the locality. In the upper parts of the outcrop it occurs as thick continuous druses of cloudy to opaque white complexly-twinned (phacolitic) crystals reaching 1.5 cm in diameter associated with earlier saponite and occasionally later calcite.

In the lower section of the exposed basalt, where the vesicle mineralogy is more varied and complex, chabazite is the last of the zeolite species to crystallise. Here it occurs as white to colourless crystals up to 1 cm across showing a variety of complex phacolitic habits as well

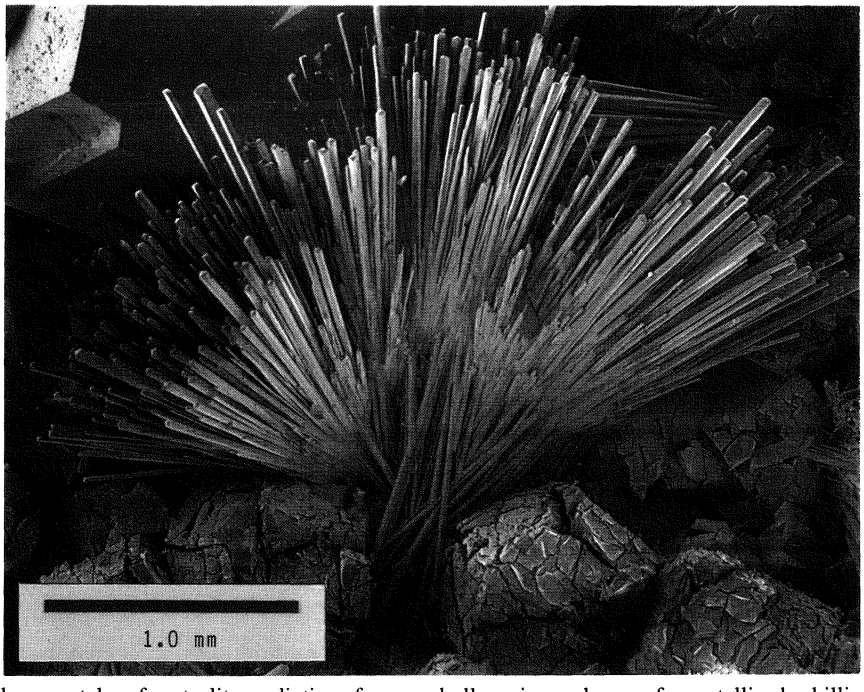

Fig.8. Acicular crystals of natrolite radiating from a hollow in a druse of crystallised phillipsite, which has decrepitated under the high vacuum conditions of the SEM. Scanning electron micrograph, secondary electron image. Author's specimen and micrograph.

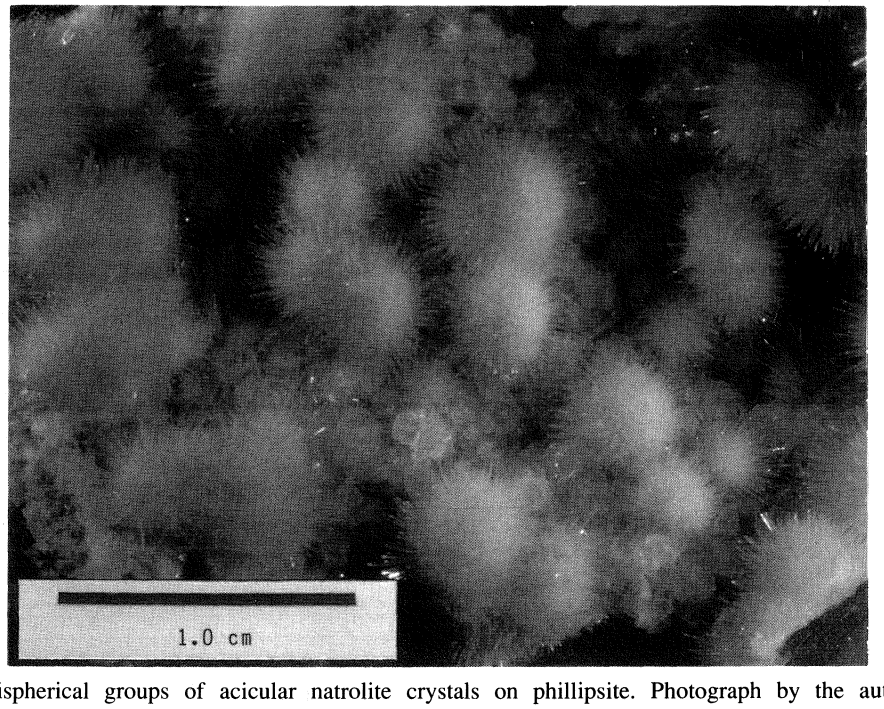

Fig.9. Hemispherical groups of acicular natrolite crystals on phillipsite. Photograph by the author.

as simple interpenetrant rhombohedra of the form r{10$\bar{1}$1} with the c-axis as the twin axis (Figs 6, 7). Crystals are commonly penetrated by earlier natrolite and calcite. The smaller crystals are unusually transparent.

Natrolite $Na_2Al_2Si_3O_{10}.2H_2O$ (Zeolite Group)

Natrolite is one of the most abundant vesicle-lining zeolites at this locality but its occurrence is restricted to the lower part of the outcrop. It commonly occurs as groups of thin prismatic colourless crystals up to 4 mm in length radiating from hollows in phillipsite druses (Fig.8). Groups are usually partly overgrown by radiate globular saponite, particularly at their base, and also by later chabazite. In some vesicles natrolite occurs as hemispherical groups (Fig.9) or jackstraw masses

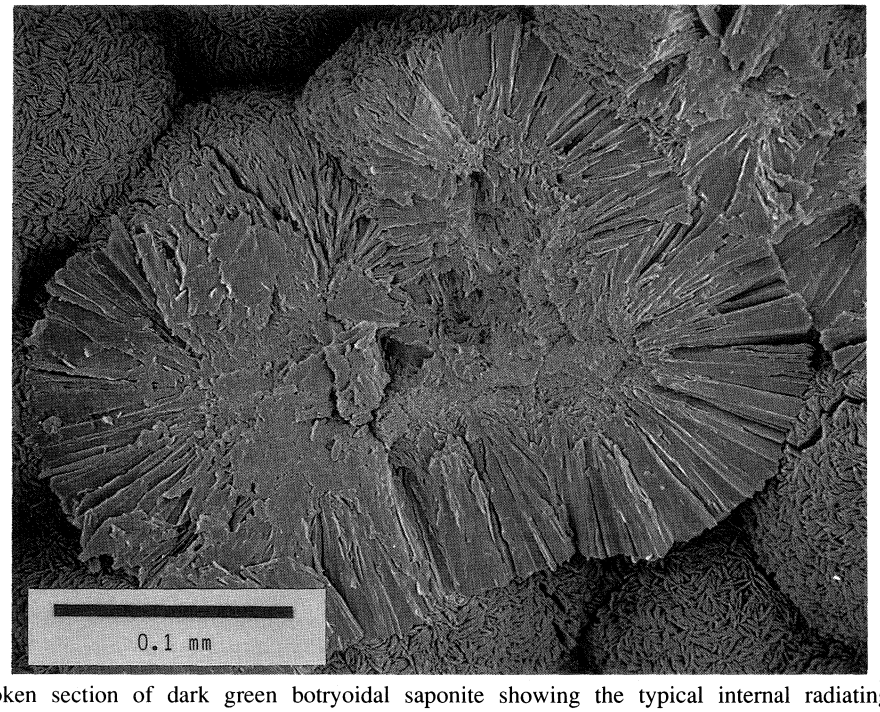

Fig.10. Broken section of dark green botryoidal saponite showing the typical internal radiating structure. Scanning electron micrograph, secondary electron image. Author's specimen and micrograph.

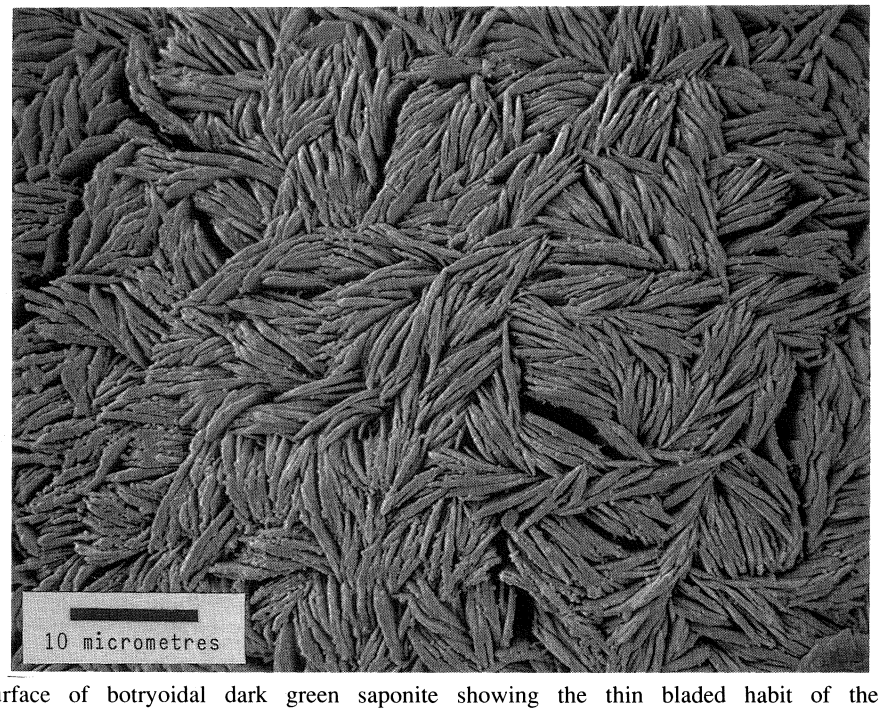

Fig.11. Surface of botryoidal dark green saponite showing the thin bladed habit of the component crystallites. Scanning electron micrograph, secondary electron image. Author's specimen and micrograph.

of acicular crystals. Crystals of different size characteristics are occasionally present in the same vesicle, suggesting different episodes of crystallisation.

Crystals are simple in habit, comprising the forms m{110} and p{111}. The p faces are commonly offset, occasionally resulting in only one adjacent pair of faces on the termination.

Saponite $(Ca/2,Na)_{0.3}(Mg,Fe^{2+})_3(Si,Al)_4O_{10}(OH)_2.4H_2O$

This trioctahedral smectite is ubiquitous throughout the sequence as a result of hydrothermal alteration of the basalt mesostasis and occurs in two distinctly different habits.

In the upper chabazite-rich zone it is abundant as massive fine-grained sectile material preceding chabazite deposition and completely filling smaller vesicles. Larger

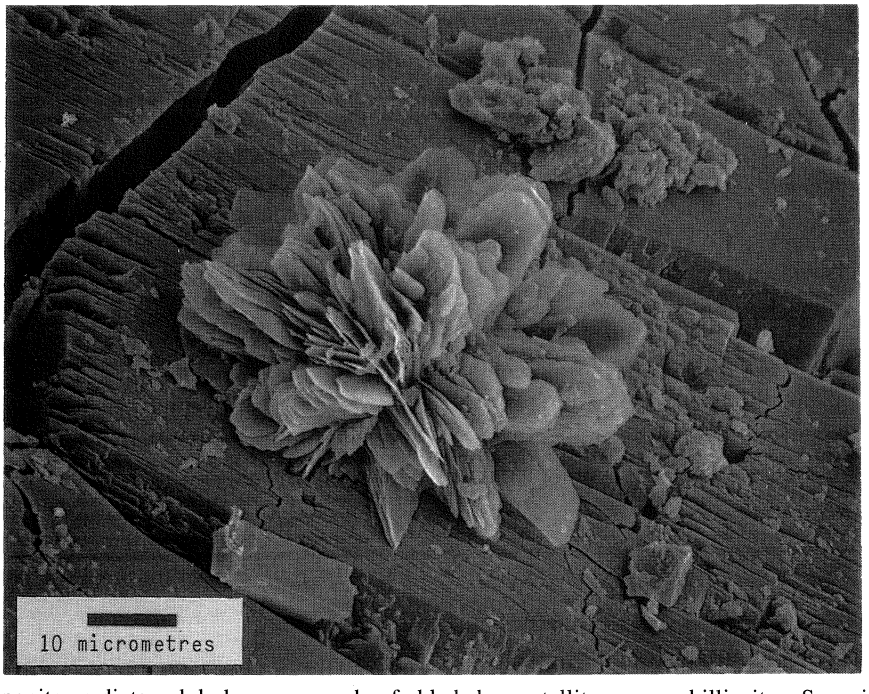

Fig.12. Saponite radiate globule composed of bladed crystallites, on phillipsite. Scanning electron micrograph, secondary electron image. Author's specimen and micrograph.

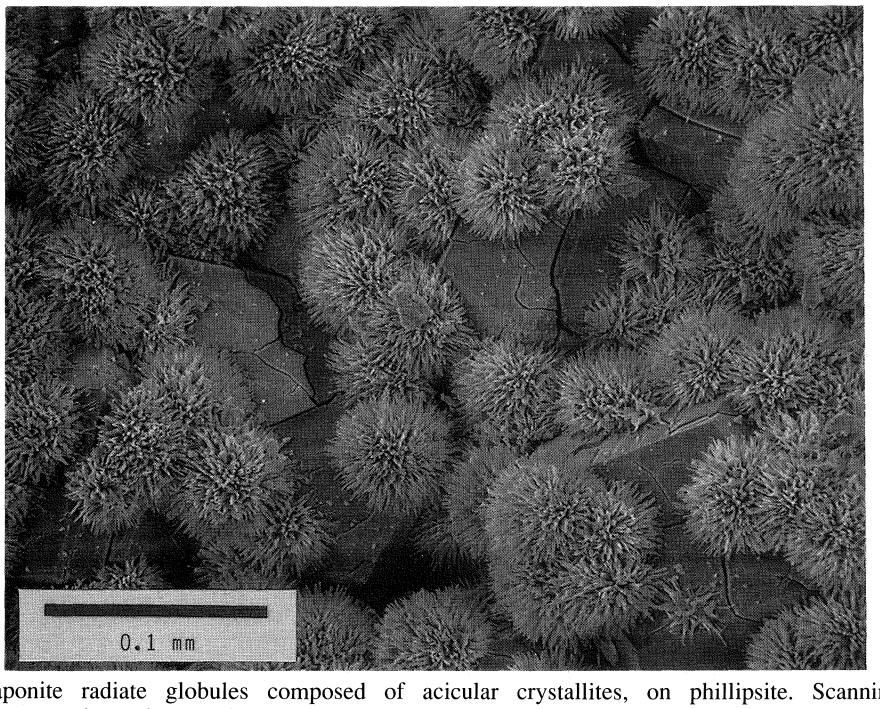

Fig.13. Saponite radiate globules composed of acicular crystallites, on phillipsite. Scanning electron micrograph, secondary electron image. Author's specimen and micrograph.

vesicles are lined with an irregular selvedge of saponite up to 1 cm thick. It also occurs as scattered irregular variegated masses up to 10 cm or more across in the vicinity of the laterally continuous lenticular cavities already described.

Colour varies from dark green (almost black) to a pale apple green and almost white. Small scale rhythmic layering is common, with alternating dark and light bands. This colour zoning is remarkably consistent between vesicles and often the colour sequence is repeated more than once in the same vesicle.

Massive saponite appears to be rare below the chabazite zone. Here the mineral occurs as scattered individual radiate globules from 0.05 to 0.2 mm in diameter or botryoidal groups up to 4 mm across deposited over phillipsite crystals. The amount present varies markedly between adjacent vesicles, although continuous crusts are rare. Radiate globules are often

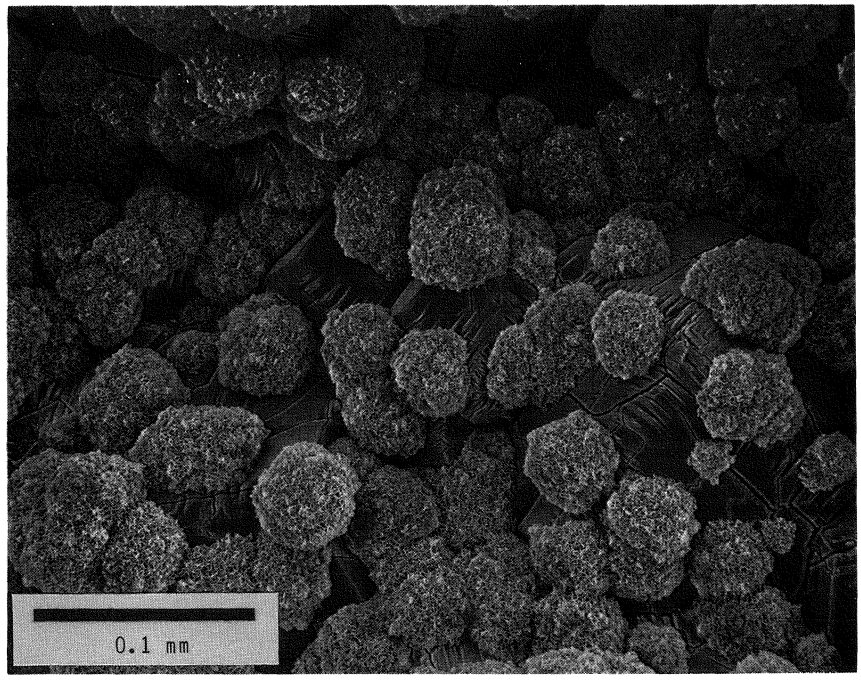

Fig.14. Spherules of fibrous matted saponite on phillipsite. Scanning electron micrograph, secondary electron image. Author's specimen and micrograph.

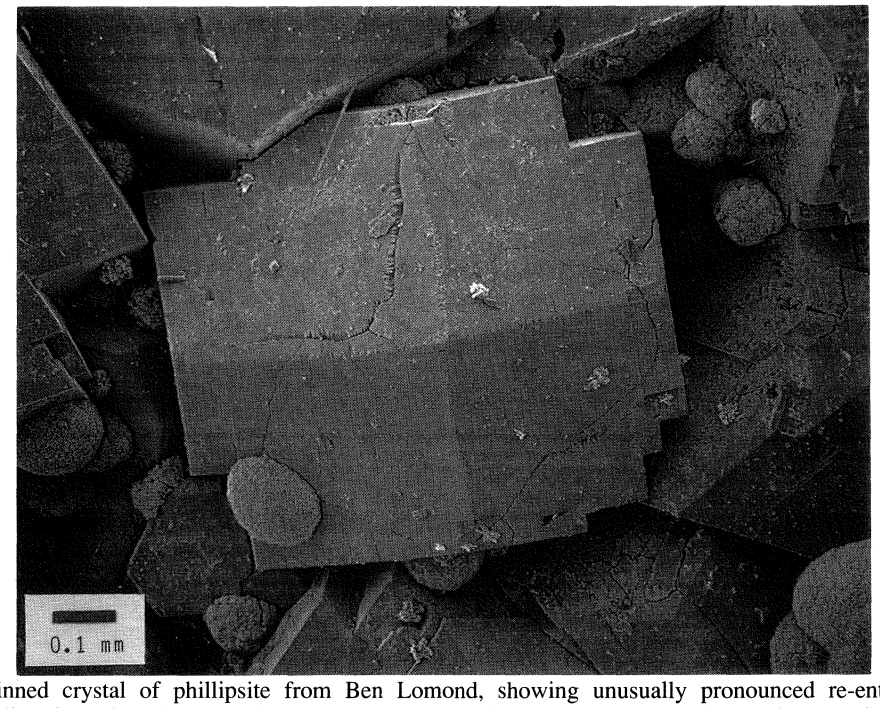

Fig.15. Twinned crystal of phillipsite from Ben Lomond, showing unusually pronounced re-entrant angles for this locality. Scanning electron micrograph, secondary electron image. Author's specimen and micrograph.

nucleated preferentially around the base of natrolite groups and partially envelop earlier aragonite and calcite. Colour of the saponite varies from an attractive pale translucent green to very dark green, almost black.

Morphology of the crystallised saponite varies considerably. The more extensive dark green botryoidal coatings comprise radiating masses of thin bladed crystals (Figs 10, 11). Crystallites making up the scattered individual radiate globules vary from bladed (Fig.12) to acicular (Fig.13) and occasionally fibrous matted (Fig.14). The acicular forms show an unusually high lustre.

XRD scans of massive pale green material from the chabazite zone and dark green radiate globular crystal groups from the phillipsite zone show the diagnostic 060 reflection to occur at 1.532A and 1.540A respectively, in very close agreement with a near normal saponite-15A from Skye, Scotland (JCPDS card 29-1491), and a ferroan saponite-15A from Cauenga Pass, California (JCPDS card 13-305). These d spacings also fall within the range given by Grim (1953) for the trioctahedral smectites (1.525A-1.535A). In the dioctahedral subgroup (which includes nontronite) the 060 reflection generally occurs at around 1.500A.

Phillipsite $(K,Na,Ca)_{1-2}(Si,Al)_8O_{16}.6H_2O$ (Zeolite Group)

Phillipsite was the first of the zeolites to crystallise, although it is absent from the upper part of the outcrop, occurring only below the zone of laterally continuous lenticular cavities. It forms colourless or partly cloudy to opaque white complexly twinned crystals (Fig.15) usually less than 1 mm but occasionally up to 3 mm across.

The forms present include c{001}, m{110} and b{010}, although faces of the form b{010} are generally insignificant or occasionally absent. The form a{100} has not been observed on crystals from this locality. Crystals are twinned on c{001} and then multiply twinned on e{011} to produce cruciform habits (Fig.16),

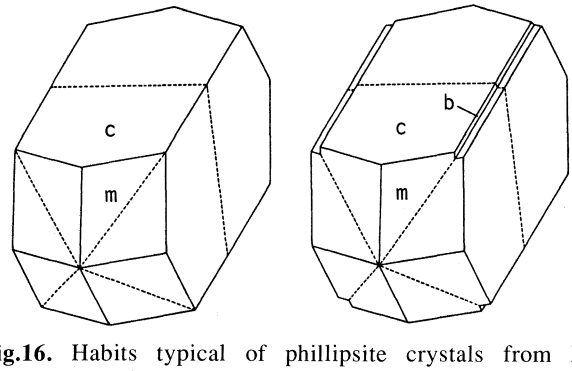

Fig.16. Habits typical of phillipsite crystals from Ben Lomond. Drawings by the author (modified from Goldschmidt, 1922).

which are rarely obvious due to the small size of the re-entrant angles. At first glance crystals commonly resemble tetragonal prisms terminated by pyramidal faces. Only rarely are opposing striations present on adjacent m faces.

Partial dissolution of phillipsite crystals is common at Ben Lomond, especially in the presence of later radiate globular saponite. Leaching took place initially at the vesicle/basalt interface and spread inwards towards the centre of the vesicles, resulting in extensive internal cavity networks and occasionally etched crystal faces. Where this has occurred, the earlier crystals are accompanied by a later generation of larger unaltered crystals, deposited over the radiate globular saponite. These later crystals characteristically show a variety of unusual distorted habits (Fig.17).

The earlier-deposited phillipsite dehydrates rapidly and decrepitates under the high vacuum conditions in the SEM (see Fig.8), so that examination of crystals by this technique is difficult.

Levyne-Offretite $(Ca,Na_2,K_2)Al_2Si_4O_{12}.6H_2O$ and $(K_2,Ca)_5Al_{10}Si_{26}O_{72}.30H_2O$ (Zeolite Group)

Thin tabular levyne crystals with offretite overgrowths have been reported in a single small specimen collected from rubble on the quarry floor. The minerals occurred alone on the specimen so that the position of these species in the paragenesis and their relationship to the alteration zones observed at the locality is not known.

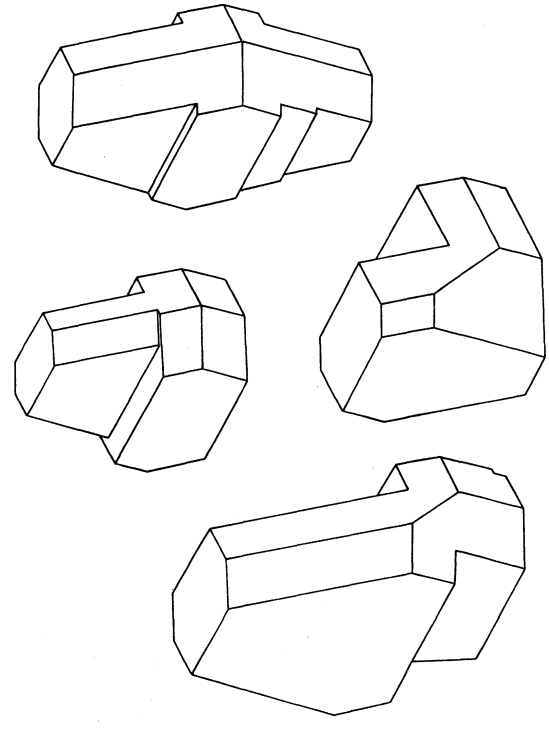

Fig.17. Crystal distortions typical of second generation phillipsite from Ben Lomond. Drawings by the author.

Chemical Composition of Zeolites and Other Secondary Minerals – Analytical Technique

Polished sections of the zeolites and other secondary minerals from various locations within the exposed basalt were chemically analysed using an EDAX Model PV9100/65 energy dispersive X-ray spectrometer (EDS) attached to a Philips SEM 505 scanning electron microscope (SEM). The analyses were performed using an accelerating voltage of 14.00 KV, beam current 2.00 nA, tilt angle 0.0°, and take-off angle of 25.5°. Standards used were: albite (Na), MgO(Mg), kyanite (Al), wollastonite (Si and Ca) and Fe(Fe). Spectrum deconvolution, background subtraction and ZAF correction were carried out using an EDAX implementation of the NBS FRAME C program (Myklebust *et al.*, 1979) modified and extended by Russ (1979).

For the zeolite species, spectra were collected for 100 seconds over an area of approximately 1 x 0.8 mm to minimise dehydration of the analysis area by the heating effect of the electron beam. Where the presence of significant levels of sodium and potassium were suspected, a continuously scanning beam was used during each analysis to minimise volatilisation of these elements. The results of these microanalyses, excluding H_2O calculated by difference, are presented in Tables 2 to 4 (see Appendix) and Table 6 (see Appendix). Elements not reported were not detected in the EDS spectra.

Gottardi & Galli (1985) suggest discarding zeolite analyses where the 'balance error' lies outside 10%. This error is given by the equation:

$$E\% = \frac{(Al + Fe) - (Li + Na + K) - 2(Mg + Ca + Sr + Ba)}{(Li + Na + K) + 2(Mg + Ca + Sr + Ba)} \times 100$$

This test has been applied to the microanalyses presented in this paper. The concept of balance error is especially applicable to microprobe analyses where water can only be determined by difference and hence where a check on the analytical total is not possible. It is a very useful check on possible volatilisation of light elements during the analysis (Rogers & Hudson, 1992).

Chemical Composition of the Vesicle Minerals

Chabazite

Microanalyses of chabazite crystals from various locations within the basalt show little variation (Table 2 [see Appendix]). Calculated Si:(Si + Al) ratios are well within the range for hydrothermal chabazites given by Gottardi & Galli (1985), with the highest value observed being 0.72 in a crystal from the phillipsite/natrolite zone. Calcium is the dominant extra-framework cation and the potassium content of the unit cell is unusually low compared to the data of Gottardi & Galli (1985). Sodium appears to be absent from crystals within the chabazite zone, but increases down the sequence to a maximum of 0.60 weight percent Na_2O in crystals from the phillipsite/natrolite zone.

Natrolite

Apart from a slightly greater assumed water content, microanalyses of natrolite from Ben Lomond (Table 3 [see Appendix]) conform very closely to the stoichiometric formula given by Fleischer & Mandarino (1991). Calculated Si:(Si + Al) ratios for a number of crystals from different vesicles were constant at 0.61. Individual crystals show little variation, except for the presence of low calcium levels towards the base of some crystal groups. In these cases the observed Ca content of the unit cell reaches a maximum of 0.08, well within the 0.5 limit of calcium substitution for sodium given by Gottardi & Galli (1985). Potassium, if present, is below the detection limits of the EDS technique.

Natrolite crystal groups often radiate from hemispherical masses of gelatinous material of similar composition but containing significantly larger amounts of CaO (up to 1.7 weight%), apparently greater levels of hydration, and slightly higher Si:(Si + Al) ratios (Analyses 5 and 6, Table 3 [see Appendix]). Compared to the natrolite crystals, relatively high E% values calculated from analyses of this material suggest that significant amounts of sodium have been preferentially leached from these areas. The presence of calcium in excess of the maximum allowable unit cell content for natrolite suggests the possible presence of small amounts of intermixed calcite.

Saponite

Microanalyses of material from several sites within the mineralised zone (Table 4 [see Appendix]) show a wide variation in composition, especially in terms of iron content. The analyses are consistent with saponite, with the X-sites containing Ca but little detectable Na and the Y-sites dominated by Mg [Mg/Mg + Fe = 0.61 - 0.79].

In the upper chabazite-rich zone, where saponite often shows very distinct colour banding, the colour of the individual bands is directly related to their chemistry. Light green bands correlate with low iron/high magnesium and a high assumed water content, while the dark bands contain high iron/low magnesium and significantly lower assumed levels of hydration.

Wide compositional variations are also evident in radiate globular saponite from the phillipsite zone and lower down the sequence. Here, the smaller radiate globules tend to be Mg-rich and pale green in colour, while the larger radiate globules are higher in iron and dark green to almost black.

Determination of Fe^{2+} and total iron by titration methods (Table 5 [see Appendix]) suggests that the amount of Fe^{3+} occupying octahedral positions is fairly constant over the range in compositions observed. However the Fe^{2+} content varies considerably, from relatively minor levels in pale green massive material from the chabazite zone to the major iron species in dark green radiate globular material from the phillipsite zone.

Phillipsite

Microanalyses of phillipsite crystals (Table 6 [see Appendix]) clearly show the presence of two distinct growth episodes. In comparison to the initial phillipsite crusts, later crystals show a significantly greater Si content in the unit cell, with the proportion of Si atoms in the tetrahedra reaching 75%, compared to a maximum of 66% in crystals from the initial growth period. Accompanying the higher Si is a higher Na content as well as lower Ca and K. The Ca content in some of the earlier crystals is close to the maximum observed in phillipsite (Gottardi & Galli, 1985). Calculated E% values for the analyses suggest that very little Na or K has been lost by volatilisation.

Whereas the earlier phillipsite crystals dehydrate and decrepitate rapidly under the high vacuum of the SEM, crystals from the second generation appear quite stable.

Discussion

As well as the zonation already described, several other significant and consistent observations have been made concerning the alteration of the basalt and secondary mineral associations.

1. The degree of hydrothermal alteration in the upper part of the quarry face appears to be directly related to the abundance of chabazite in the vesicles. Where chabazite is absent, there is very little obvious proximal development of smectite alteration products. This suggests a direct relationship between the intensity of hydrothermal alteration and chabazite deposition.

2. Even though the basalt in the phillipsite and phillipsite/natrolite zones is extensively altered, vesicle linings are only occasionally preceded by a very thin (less than 1 mm) selvedge of saponite.

3. Alteration within both the phillipsite and phillipsite/natrolite zones appears to have developed uniformly throughout the basalt, with little evidence for concentration of hydrothermal fluids around cooling cracks, vesicles, or other irregularities. This suggests the existence of fairly uniform conditions of elevated temperature and high pore water pressure over a significant time period.

4. Near the top of the outcrop, where chabazite and saponite are the only secondary minerals present, earlier saponite is often present as horizontally-layered deposits immediately adjacent to the basalt at the base of the smaller vesicles. In the lower part of the outcrop, where chabazite is preceded by phillipsite and then phillipsite-natrolite associations, similar deposits of saponite occur occasionally, but these postdate both phillipsite and natrolite and predate chabazite.

5. Phillipsite is thermodynamically unstable and dissolves rapidly in the face of local changes in the depositional environment (Kastner, 1979). The ubiquitous partial leaching of earlier-formed crystals in both the phillipsite and phillipsite/natrolite zones in the presence of later radiate globular saponite therefore suggests significant changes in the vesicle environment accompanied the deposition of radiate globular saponite and preceded the crystallisation of chabazite.

6. In the lower part of the exposed basalt, a significant proportion of vesicles which contain major radiate globular saponite also contain major chabazite.

These observations suggest initial crystallisation of the phillipsite, aragonite and natrolite in vesicles within the lower part of the exposed basalt by normal deuteric processes during cooling. Deposition of this deuteric suite was followed by a second phase of hydrothermal activity which resulted in extensive alteration of the basalt and the overprinting of radiate globular saponite/chabazite/calcite associations on the earlier vesicle minerals. The observed gelatinisation and calcium enrichment at the base of natrolite sprays also appears to have taken place at this stage.

Jakobsson & Moore (1986) found that deep within the still-cooling basaltic tephra of Surtsey Volcano (Iceland), dioctahedral smectite (nontronite) had formed from the alteration of olivine phenocrysts at temperatures exceeding 115°C. The occurrence of globular habits similar to, though smaller than, those observed in saponite at Ben Lomond was restricted to vesicles in zones where the average temperature exceeded 133°C. Hence it is probable that the coarse radiate globular saponite observed in vesicles at Ben Lomond was the result of high temperatures and pore water pressures introduced by renewed hydrothermal activity and maintained by the blanketing effect of the overlying basalt.

The same episode of hydrothermal activity which produced the changes in secondary mineral associations in the lower sections of the basalt was also responsible for the extensive alteration in the upper section and the accompanying deposition of abundant saponite and chabazite.

The observed patterns of hydrothermal alteration and zonal distribution of the zeolites centre around the laterally continuous lensoidal cavities described earlier. The concentration of zeolites in such laterally extensive void systems is commonly the result of large scale movement of subsurface hot waters (Pecover, 1987) and it is very likely that these cavities represent either areas of heated entrapped meteoric water or hot spring conduits. In fact, species of the smectite group (in this case saponite) often occur as hydrothermal alteration

products near hot springs (Deer *et al.*, 1963). In either case, the upper chabazite-rich basalt appears to represent a later flow which would have acted as an effective blanket in sealing in the high temperatures and abundant water necessary to produce the alteration and additional secondary minerals observed in the lower phillipsite and phillipsite/natrolite zones located within what appears to have been an earlier flow.

The chabazite-phillipsite-natrolite associations lining vesicles and abundant massive thomsonite in what appear to have been hot spring conduits are typical of a silica-undersaturated environment (Coombs *et al.*, 1959). This explains the absence of quartz or any other form of silica in association with the zeolites at Ben Lomond.

Conclusions

Amygdaloidal basalts exposed by recent roadwork near Ben Lomond have provided an abundance of zeolites and associated secondary minerals typical of a silica-undersaturated environment.

Deposition of the vesicle minerals was controlled initially by normal deuteric processes during cooling. Additional mineralisation (including coarse radiate globular saponite and chabazite) was superimposed on the deuteric suite during a subsequent phase of hydrothermal activity associated with the development of proximal hot springs between successive basalt flows. Extensive alteration of the basalt also appears to have resulted from the action of post-deuteric hydrothermal fluids, rather than from more recent low temperature weathering processes.

The range of calcite morphologies and their individual reactions to ultraviolet light are unusual for a single locality.

ACKNOWLEDGMENTS. Appreciation is expressed to the Management, BHP Research, Newcastle Laboratories for the use of the equipment and resources of the laboratories. Jules Dubrawski ran XRD scans of the saponite and Ken Doolan provided the titration analyses. Appreciation is also expressed to Morrie Duggan for his critical review of the original manuscript and helpful suggestions. Graham Delaforce (Kingswood, NSW) provided information on the discovery of levyne/offretite at the locality.

References

Coombs, D.S., A.D. Ellis, W.S. Fyfe & A.M. Taylor, 1959. The zeolite facies, with comments on the interpretation of hydrothermal synthesis. Geochimica et Cosmochimica Acta 17: 53.

Deer, W.A., R.A. Howie & J. Zussman, 1963. The Rock Forming Minerals, Vol.3, Sheet Silicates. Longmans.

England, B.M., 1984. The paragenesis of contrasting habits of calcite and aragonite-calcite associations from Kulnura, New South Wales, Australia. Mineralogical Magazine 48(4): 519-527.

Fleischer, M. & J.A. Mandarino, 1991. Glossary of Mineral Species. The Mineralogical Record Inc., Tucson.

Goldschmidt, V., 1913. Atlas der Krystallformen, II.

Goldschmidt, V., 1922. Atlas der Krystallformen, VI.

Gottardi, G. & E. Galli, 1985. Natural Zeolites. Springer-Verlag.

Grim, R.E., 1953. Clay Mineralogy. McGraw Hill.

Jakobsson, S.P. & J.G. Moore, 1986. Hydrothermal minerals and alteration rates at Surtsey volcano, Iceland. Geological Society of America Bulletin 97: 648-659.

Kastner, M., 1979. Zeolites. Pp. 111-122. **In** R.G. Burns (ed.). Marine Minerals. Mineralogical Society of America. Short Course Notes. Vol.6.

Lebedev, L.M., 1967. Metacolloids in endogenic deposits. Plenum Press, New York.

Leitmeier, H., 1910. Zur Kenntnis der Carbonate, Die Dimorphie des Kohlensauren Kalkes. I. Teil: Neues Jahrbuch Mineralogie Abhandlungen 1: 49-74.

Leitmeier, H., 1915. Zur Kenntnis der Carbonate. II. Teil: Neues Jahrbuch Mineralogie Abhandlungen 40: 655-700.

Myklebust, R.L., C.E. Fiori & K.F.J. Heinrich, 1979. Frame C: A compact procedure for quantitative energy dispersive electron probe X-ray analysis. United States Department of Commerce, National Bureau of Standards, Washington D.C., Technical Note 1106.

Pecover, S., 1987. A review of the formation and geology of natural zeolites. Pp. 11-24. **In** Natural Zeolites. Geological Survey of New South Wales Report GS1987/145.

Rogers, K.A. & N. Hudson, 1992. Laumontite and heulandite-clinoptilolite pseudomorphs after Jurassic gastropods from Ponganui, New Zealand. Records of the Australian Museum Supplement 15: 73-81.

Russ, J.C., 1979. Modifications and extensions to NBS Frame C. Microbeam Analysis: 268-272.

Accepted November 19, 1992

APPENDIX

Table 1. Paragenesis of zeolites and associated secondary minerals from Ben Lomond, NSW.

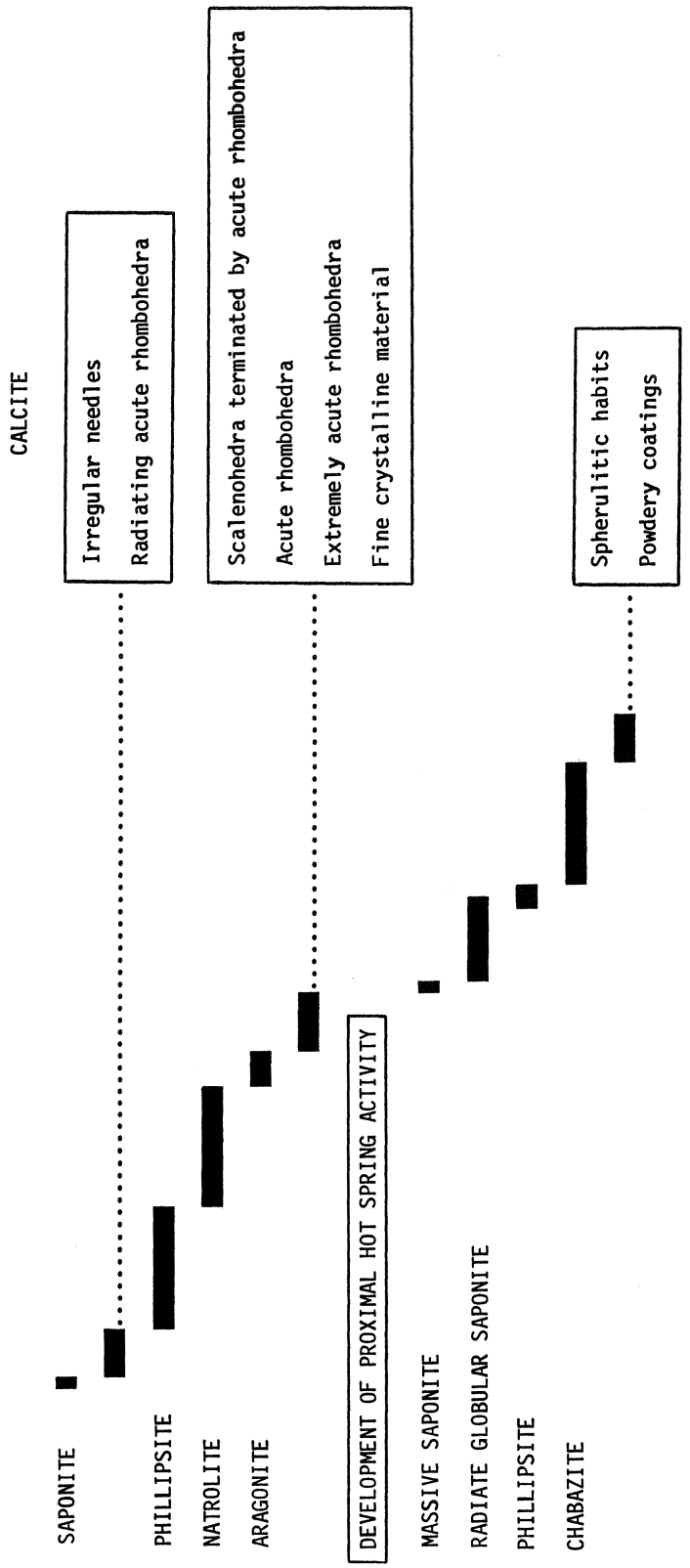

Table 2. Microanalyses of chabazite from Ben Lomond, NSW.

	1	2	3	4	5	6	7	8	9
SiO_2	49.60	50.40	48.90	52.40	53.00	52.90	51.80	52.30	51.00
Al_2O_3	18.10	17.80	18.10	18.10	18.40	17.90	17.20	17.80	18.00
CaO	9.30	9.00	9.20	9.20	9.30	8.80	8.40	8.60	8.80
Na_2O	–	–	–	–	–	0.20	0.30	0.30	0.60
K_2O	0.70	0.80	0.80	0.90	1.00	1.00	0.80	0.90	0.90
TOTAL	77.60	78.10	76.90	80.60	81.70	80.90	78.40	79.90	79.30
Cell content based on 24 oxygens.									
Si	8.40	8.51	8.36	8.54	8.54	8.57	8.64	8.57	8.47
Al	3.62	3.53	3.66	3.49	3.48	3.43	3.38	3.44	3.52
Ca	1.68	1.64	1.70	1.61	1.62	1.53	1.50	1.53	1.57
Na	–	–	–	–	–	0.04	0.09	0.09	0.17
K	0.13	0.18	0.18	0.18	0.20	0.22	0.18	0.18	0.17
E%	3.72	2.02	2.23	2.65	1.16	3.31	3.36	3.30	1.15
Si:(Si+Al)	0.70	0.71	0.70	0.71	0.71	0.71	0.72	0.71	0.71

1-3 : Chabazite Zone
4-6 : Phillipsite Zone
7-9 : Phillipsite/Natrolite Zone

Table 3. Microanalyses of natrolite from Ben Lomond, NSW.

	1	2	3	4	5	6
SiO_2	47.30	47.00	47.90	48.50	46.70	47.30
Al_2O_3	25.30	25.50	25.80	25.70	25.20	24.90
CaO	–	–	0.10	0.20	1.70	0.70
Na_2O	14.50	14.50	14.80	14.70	12.40	13.70
TOTAL	87.10	87.50	88.60	89.10	86.00	86.60
Cell content based on 80 oxygens.						
Si	24.68	24.51	24.59	24.75	24.59	24.74
Al	15.58	15.66	15.55	15.44	14.62	15.39
Ca	–	–	0.08	0.08	0.95	0.39
Na	14.73	14.97	14.75	14.51	12.67	13.95
E%	5.77	4.61	4.29	5.25	7.21	4.48
Si:(Si+Al)	0.61	0.61	0.61	0.62	0.63	0.62

1-4 : Natrolite crystal sections
5-6 : Base of natrolite sprays

Table 4. Microanalyses of saponite from Ben Lomond, NSW.

	1	2	3	4	5	6	7
SiO_2	41.50	42.50	40.50	38.80	46.30	36.70	46.50
Al_2O_3	13.20	15.50	15.70	19.00	9.60	14.40	11.90
Fe_2O_3	12.60	8.00	11.78	19.67	12.60	20.20	14.50
MgO	19.70	19.80	16.60	17.00	18.80	15.90	17.70
CaO	1.50	1.80	1.50	1.40	1.20	0.60	0.80
Na_2O	–	–	–	0.30	–	–	–
K_2O	0.10	–	–	–	–	–	–
TOTAL	88.60	87.60	86.08	96.17	88.50	87.80	91.40

Cell content based on 22 oxygens.

Si	6.02	6.12	6.02	5.33	6.75	5.51	6.47
Al	2.26	2.63	2.74	3.05	1.66	2.55	1.96
Fe	1.38	0.87	1.31	2.02	1.38	2.28	1.53
Mg	4.26	4.23	3.66	3.45	4.08	3.57	3.69
Ca	0.23	0.28	0.24	0.21	0.20	0.11	0.13
Na	–	–	–	0.07	–	–	–
K	0.02	–	–	–	–	–	–

1. Initial saponite selvedge from Phillipsite zone.
2. Pale green saponite from Chabazite zone.
3. Mid green saponite from Chabazite zone.
4. Dark green saponite from Chabazite zone.
5-7. Dark green spherulitic saponite from Phillipsite zone.

Table 5. Analysis of iron species in Ben Lomond saponite.

	1	2	3
FeO	1.03	6.00	7.81
$Fe_2O_3^*$	4.20	4.26	4.21
Fe^{3+}/Fe^{2+}	3.68	0.64	0.49

* Determined by: 1.429730 (Fe_{Total} - Fe^{2+})

1. Pale green massive saponite from chabazite zone
2-3. Dark green radiate globular saponite from phillipsite zone.

Table 6. Microanalyses of phillipsite from Ben Lomond, NSW.

	1	2	3	4	5	6	7
SiO_2	46.10	44.80	46.10	45.90	46.60	53.70	52.80
Al_2O_3	21.20	20.20	20.90	20.70	21.50	17.70	18.20
CaO	8.00	7.80	7.90	7.90	8.30	6.30	6.40
Na_2O	0.10	0.10	0.20	0.10	–	1.40	1.40
K_2O	5.80	5.50	5.60	5.60	5.70	3.40	3.70
TOTAL	81.30	78.40	80.80	80.20	82.20	82.40	82.50
Cell content based on 32 oxygens.							
Si	10.42	10.44	10.44	10.48	10.37	11.55	11.40
Al	5.62	5.56	5.59	5.53	5.65	4.46	4.61
Ca	1.93	1.96	1.93	1.91	2.00	1.45	1.49
Na	0.06	–	0.12	0.06	–	0.56	0.62
K	1.70	1.65	1.63	1.65	1.61	0.93	1.03
E%	0.00	-0.18	-0.36	0.00	0.71	1.59	-0.43
Si:(Si+Al)	0.65	0.65	0.65	0.65	0.65	0.72	0.71

1-5 : Crystals from Phillipsite Zone
6-7 : Second generation crystals from phillipsite/natrolite zone.

Full-text PDF of each one of the works in this volume are available at the following links :